33rd Annual International Conference of the IEEE EMBS
Boston, Massachusetts USA, August 30 - September 3, 2011

Tracking the Changes of Hippocampal Population Nonlinear Dynamics in Rats Learning a Memory-Dependent Task

Rosa H. M. Chan, *Student Member, IEEE*, Dong Song, *Member, IEEE,*
Anushka V. Goonawardena, Sarah Bough, John Sesay, Robert E. Hampson, Sam A. Deadwyler, and
Theodore W. Berger, *Fellow, IEEE*

***Abstract*—Neurobiological processes associated with learning are known to be highly nonlinear, dynamical, and time-varying. Characterizing the time-varying functional input-output properties of neural systems is a critical step to understand the neurobiological basis of learning. In this paper, we present a study on tracking of the changes of neural dynamics in rat hippocampus during learning of a memory-dependent delayed nonmatch-to-sample (DNMS) task. The rats were first trained to perform the DNMS task without a delay between the sample and response events. After reaching a performance level, they were subjected to the DNMS task with variable delays with a 5s mean duration. Spike trains were recorded from hippocampal CA3 (input) and CA1 (output) regions during all training sessions and constitute the input-output data for modeling. We applied the time-varying Generalized Laguerre-Volterra Model to study the changes of the CA3-CA1 nonlinear dynamics using these data. Result showed significant changes in the Volterra kernels after the introduction of delays. This result suggests that the CA3-CA1 nonlinear dynamics established in the initial training sessions underwent a functional reorganization as animals were learning to perform the task that now requires delays.**

I. Introduction

Tracking the changes of neural nonlinear dynamics using neuronal spiking activities is a critical step to understand the neurobiological basis of learning from behaving animals. It allows us to bridge the gap between the behavior and the well-known forms of neural plasticity, such as long-term potentiation (LTP) and long-term depression (LTD). For example, it has been shown that LTP induced by high-frequency stimulation to the perforant path of the hippocampus accelerates subsequent classical conditioning [1]. LTP was also observed *in vivo* in hippocampal CA1 pyramidal cells during an inhibitory avoidance task [2], demonstrating that activities generated from a real learning task were sufficient for eliciting LTP. On the other hand, it is shown that functional cell types were formed and recruited in the hippocampus during learning of a delayed-nonmatch-to-sample (DNMS) task [3]. It suggested that the changes in animal behavior at the beginning of training might be caused by the changes in the cell's firing activities. However, how the input-output properties of hippocampal regions change during learning remains unclear. The goal of this study is to characterize such changes using a recently developed quantitative modeling tools.

Specifically, we applied Generalized Laguerre-Volterra model to study the underlying nonlinear dynamics between multiple neuronal units by observing spike train inputs and outputs only [4, 5]. Eden *et al*. proposed the stochastic state point-process filter (SSPPF) [6], which updates model coefficients in proportion to the difference between the occurrence of an actual spike and the estimated probability of its occurrence. They have applied SSPPF to reconstruct monkey hand movement trajectories from a dynamic ensemble of spiking motor cortical neurons [7]. We later applied SSPPF to our established nonlinear dynamical modeling framework to track time-varying systems [8, 9]. The integrated method was tested with synthetic simulations.

Here we applied the integrated method to study the neural dynamics when the behaving animals were learning to perform the memory-dependent DNMS task. Hippocampal CA3 and CA1 cells were shown to be encoding the required spatial and temporal information to complete this task [10]. We recorded spike trains from the CA3 and CA1 regions while the animals were learning the task. We will present the changes observed in the model derived from these experimental data.

II. Methods

A. Experimental Procedures

Spike trains were recorded multi-electrode arrays from different septo-temporal regions of the hippocampus of rats trained with the DNMS task [3]. For each hemisphere of the brain, an array of electrodes was surgically implanted into the hippocampus, with eight electrodes in the CA3 input region and eight electrodes in the CA1 output region. The rats were first trained to perform the DNMS task without delay, that is, they were learning to press the lever opposite to the sample lever immediately after the sample lever was presented, as in sessions 29 to 31 of Fig. 1. And then delay intervals were introduced between the sample phase and nonmatch phase, as in sessions 32 to 35 of Fig. 1. Action potentials of individual neurons were isolated by time-amplitude window discrimination and computer-identified individual waveform characteristics using a multi-neuron acquisition processor (Plexon, Dallas, TX). Only spike

Manuscript received March 26, 2011.

R. H. M. Chan, D. Song and T. W. Berger are with the Center for Neural Engineering, Department of Biomedical Engineering, University of Southern California, Los Angeles, CA 90089 USA (e-mail: homchan@usc.edu; dsong@usc.edu; berger@bmsr.usc.edu).

A V. Goonawardena, S. Bough, J. Sesay, R. E. Hampson and S. A. Deadwyler are with the Department of Physiology and Pharmacology, Wake Forest University, School of Medicine, Winston-Salem, NC 27157 USA (email: agoonawa@wfubmc.edu; sbough@wfubmc.edu; jsesay@wfubmc.edu; rhampson@wfubmc.edu; sdeadwyl@wfubmc.edu).

trains with waveforms consistent across sessions were included in analyses [3].

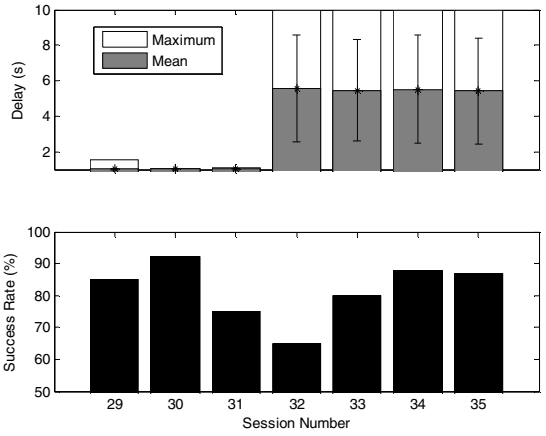

Fig. 1 Performance of animal 1150 trained with different delay intervals.

B. Generalized Volterra Model

In order to analyze the nonlinear dynamics underlying spike train transformations, a multiple-input, multiple-output (MIMO model) first was constructed using a generalized Laguerre-Volterra kernel method [4, 5]. A MIMO system was decomposed into a series of multiple-input, single-output systems (MISO). *P(t)* is the estimated firing probability of the output:

$$P(t) = 0.5 - 0.5erf\left(\frac{\theta - u(t) - a(t)}{\sqrt{2}\sigma}\right), \tag{1}$$

where *erf* is the error function; *u* is the "synaptic potential"*;* *a* is the after potential*;* θ is the threshold; and σ is the noise variance. Consider the second order Volterra self-kernel model where *N* is the total number of inputs and $\{k_0, k_1, k_{2s}\}$ are the Volterra kernels, *u* can be expressed as:

$$\begin{aligned} u(t) = k_0 &+ \sum_{n=1}^{N}\sum_{\tau=0}^{\infty} k_1^{(n)}(\tau)x_n(t-\tau) \\ &+ \sum_{n=1}^{N}\sum_{\tau_1=0}^{\infty}\sum_{\tau_2=0}^{\infty} k_{2s}^{(n)}(\tau_1,\tau_2)x_n(t-\tau_1)x_n(t-\tau_2) \end{aligned} \tag{2}$$

After potential *a* can be rewritten as $a(t) = [h * y](t)$, where *h* is the linear feedback kernel. Both feedforward kernels *k* and the feedback kernel *h,* are expanded with orthonormal Laguerre basis functions. Stochastic state point process filter is applied to estimate and track the Laguerre coefficient over time [6]. Single pulse response functions (r_1) of each input can be derived as $r_1^{(n)}(\tau) = \hat{k}_1^{(n)}(\tau) + \hat{k}_{2s}^{(n)}(\tau,\tau)$. r_1 is the response in *u* elicited by a single spike from the input neuron as a function of delay τ. To describe the joint nonlinear effects of pairs of spikes from the input neuron in addition to the first order responses, paired-pulse response functions (r_2) are expressed as a function of the delay of previous spikes, $r_2^{(n)}(\tau_1,\tau_2) = 2\hat{k}_{2s}^{(n)}(\tau_1,\tau_2)$.

C. Laguerre Expansion

The Laguerre-expansion Volterra (LEV) kernel modeling technique was used to reduce the number of open parameters to be estimated, and to separate system nonlinearities from system dynamics. Using the LEV technique, both feedforward kernels, *k*, and the feedback kernel, *h,* are expanded with orthonormal Laguerre basis functions, *b,* with input and output spike trains *x* and *y* convolved with *b*, $v_j^{(n)} = b_j * x_n$ and $v_j^{(h)} = b_j * y$. Synaptic potential, *u,* and after-potential, *a,* can be re-written into:

$$\begin{aligned} u(t) = c_0 &+ \sum_{n=1}^{N}\sum_{j=1}^{L} c_1^{(n)}(j)v_j^{(n)}(t) \\ &+ \sum_{n=1}^{N}\sum_{j_1=1}^{L}\sum_{j_2=1}^{j_1} c_{2s}^{(n)}(j_1,j_2)v_{j_1}^{(n)}(t)v_{j_2}^{(n)}(t) \end{aligned} \tag{3}$$

and

$$a(t) = \sum_{j=1}^{L} c_h(j)v_j^{(h)}(t). \tag{4}$$

Using Laguerre expansion, *v* can be computed recursively at each time *t* [9]. Let $\mathbf{V}^{(n)}(t) = [v_1^{(n)}(t) \quad \dots \quad v_L^{(n)}(t)]$,

$$\mathbf{V}^{(v)}(\mathbf{t})\mathbf{A_1} = \mathbf{V}^{(n)}(\mathbf{t-1})\mathbf{A_2} + \sqrt{1-\alpha_n^2}\,\mathbf{A_3}x_n(\mathbf{t}), \tag{5}$$

where $\mathbf{A_1} = \mathbf{I} + \alpha_n \mathbf{I}_+$; $\mathbf{A}_2 = \alpha_n \mathrm{I} + \mathrm{I}_+$; $\mathbf{A_3} = [1 \quad 0 \quad \dots \quad 0]$; **I** is an *LxL* identity matrix and $\mathbf{I}_+$ is an upper shift matrix. The convolved functions *v* include the temporal dynamics and thus *u* and *a* can be readily calculated based on the present values of *v* and the model coefficients.

D. Parameter Estimation

By the stochastic state point-process filtering algorithm [6], coefficient vector *C(t)* and its covariance matrix *W(t)* are updated iteratively at each time step *t* [8] :

$$\begin{aligned} W(t)^{-1} = [W(t-1)+Q]^{-1} + \Bigg[&\left(\frac{\partial \log P(t)}{\partial c(t)}\right)' P(t)\left(\frac{\partial \log P(t)}{\partial c(t)}\right) \\ &- (y(t)-P(t))\frac{\partial^2 \log P(t)}{\partial c(t)\partial c(t)'}\Bigg] \end{aligned} \tag{6}$$

$$C(t) = C(t-1) + W(t)\left[\left(\frac{\partial \log P(t)}{\partial C(t)}\right)'(y(t)-P(t))\right] \tag{7}$$

III. Results

We have analyzed the spike train data recorded from CA3 and CA1 of animals learning the DNMS task. In addition, we tracked changes in the underlying nonlinear neural dynamics described by the single pulse response functions r_1, paired-pulse response functions r_2, and the linear feedback *h* with a 2ms time resolution. For example, we have tracked the time-varying CA3-CA1 dynamics of animal #1150 with an 11-input, 8-output second order model. Fig. 2 shows its changes in feedback kernels $h(\tau)$ of output Neuron #45 across experimental time from sessions with no delay to sessions with new delay intervals. The x-axis represents experimental time; the y-axis represents the time lag τ between the previous input events and the present time; and

the z-axis represents the value of h. Significant kernel changes at the session when delay was first introduced. This may correspond to the change in neuron output firing properties after the introduction of 5s delay.

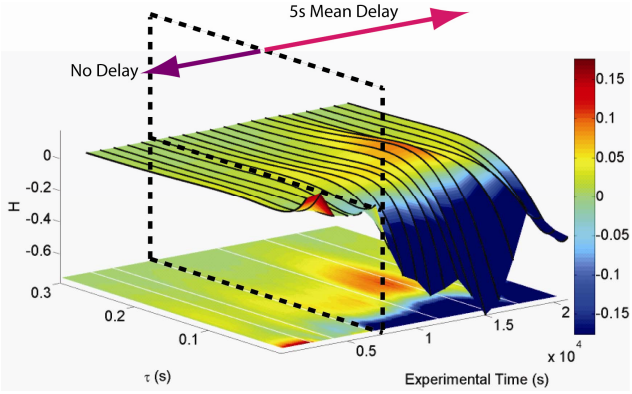

Fig. 2 Feedback kernels of output Neuron #45 across sessions.

Exemplary single pulse response functions $r_1(\tau)$ of animal #1150 are plotted in Fig. 3. Each row in Fig. 3a and Fig. 3b represents a time-varying r_1 of one input to the outputs Neuron #45 and Neuron #81 respectively. The x-axis represents experimental time; y-axis represents the time lag τ between the previous input events and the present time. Values of the response functions are color-coded, where red represents high values and blue represents low values. Results show that, during the sessions with 0 delay (i.e., sessions #29, #30 and #31), magnitudes of r_1 are small and nearly constant. When the delay is introduced to the training at session #32, magnitudes of r_1 start to increase significantly in most of the inputs, showing that the CA3-CA1 dynamics changes during the training process. The changes in r_1 persist in the following sessions (#33 to #35). Response functions of some inputs eventually converge in the later sessions, such as those of input #97 and input #121 as shown in Fig. 3a. We have also examined the learning induced changes in the paired-pulse response functions $r_2(\tau,\tau+\Delta)$ at different interspike intervals Δ as shown in Figure 4. Each row in Fig. 4 represents a time-varying r_2 of one input to the output Neuron #45. The x-axis represents experimental time; y-axis represents the time lag τ between the previous input interspike interval and the present time. Values of r_2 are color-coded, where red represents high values and blue represents low values. At output CA1 Neuron #45, the results clearly revealed the remarkable increase in the second order nonlinear properties with the introduction of delay-demanding memory at session #32.

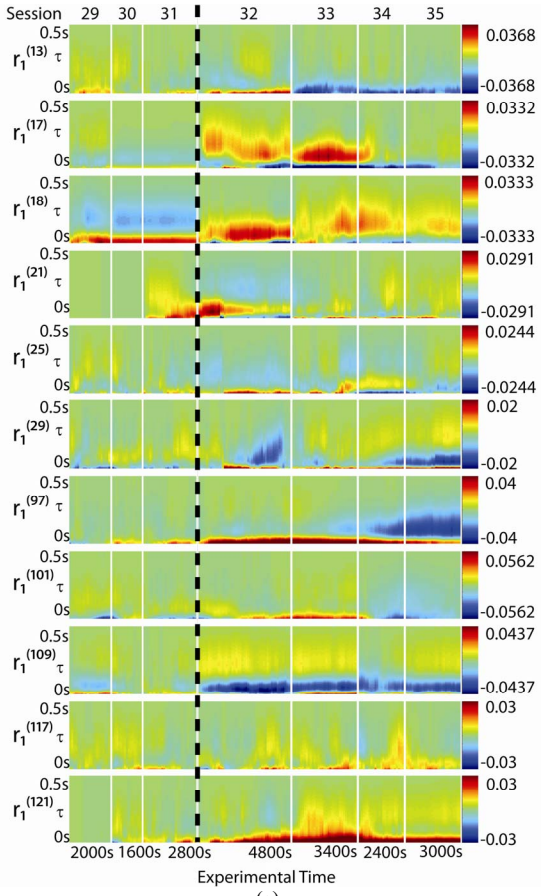

(a)

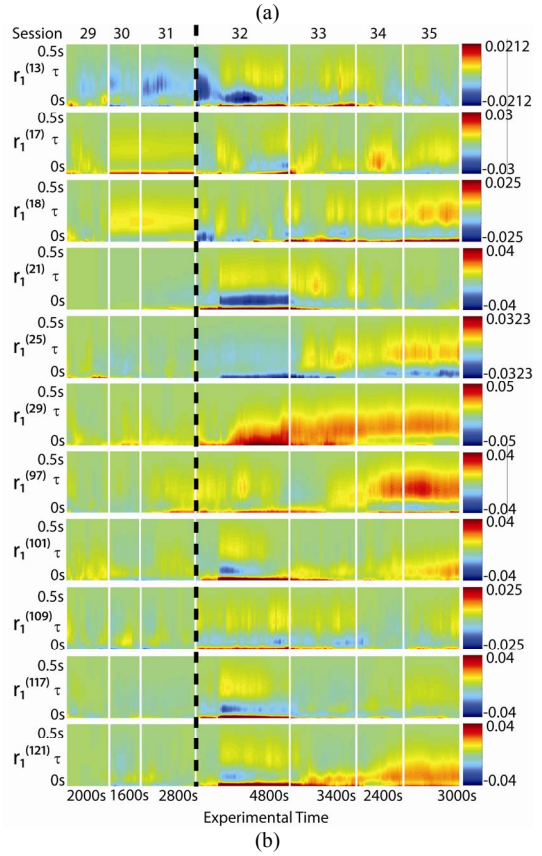

(b)

Fig. 3 Single pulse response functions $r_1(\tau)$ of a) Neuron #45 and b) Neuron #81 of animal #1150 tracked across sessions.

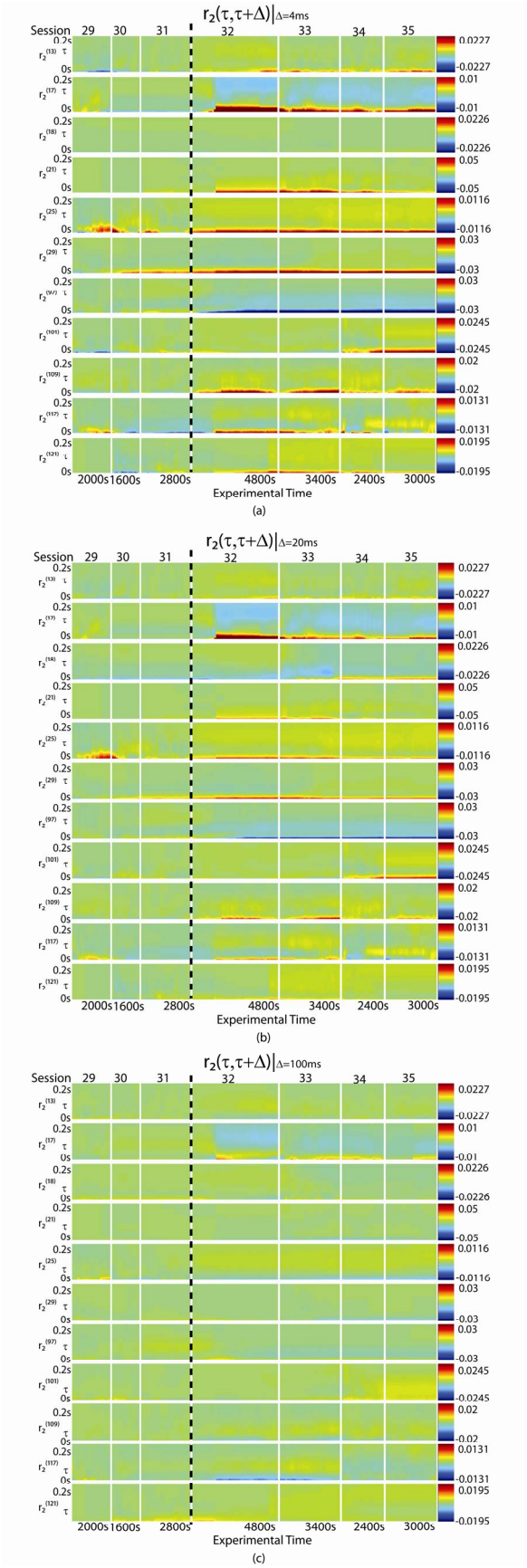

Fig. 4 Paired-pulse response $r_2(\tau,\tau+\Delta)$ to Neuron #45 as function of delay tracked across sessions when interspike interval Δ is a) 4ms, b) 20ms and c) 100ms.

IV. Discussion

The changes in estimated kernels are consistent with our preliminary results of piece-wise non-stationary modeling on the same dataset [11], and provide much more comprehensive information that allows us to study the fine details of the temporal evolutions of the CA3-CA1 nonlinear dynamics, i.e., within-session changes of the response functions in a millisecond scale. Results suggest that the model established in the initial training sessions is undergoing reconfiguration as the animal learns how to perform the task when the delays are introduced. We are visualizing, in high temporal resolutions, the encoding the short-term memory into long-term memory with the development of input-output functions.

References

[1] T. W. Berger, "Long-term potentiation of hippocampal synaptic transmission affects rate of behavioral learning," *Science,* vol. 224, pp. 627-630, 1984.

[2] J. R. Whitlock, A. J. Heynen, M. G. Shuler, and M. F. Bear, "Learning induces long-term potentiation in the hippocampus," *Science,* vol. 313, pp. 1093-1097, Aug 25 2006.

[3] A. V. Goonawardena, L. Robinson, G. Riedel, and R. E. Hampson, "Recruitment of Hippocampal Neurons to Encode Behavioral Events in the Rat: Alterations in Cognitive Demand and Cannabinoid Exposure," *Hippocampus,* vol. 20, pp. 1083-1094, 2010.

[4] D. Song, R. H. M. Chan, V. Z. Marmarelis, R. E. Hampson, S. A. Deadwyler, and T. W. Berger, "Nonlinear modeling of neural population dynamics for hippocampal prostheses," *Neural Networks,* vol. 22, pp. 1340-1351, Nov 2009.

[5] T. W. Berger, D. Song, R. H. M. Chan, and V. Z. Marmarelis, "The Neurobiological Basis of Cognition: Identification by Multi-Input, Multioutput Nonlinear Dynamic Modeling," *Proceedings of the IEEE,* vol. 98, pp. 356-374, Mar 2010.

[6] U. T. Eden, L. M. Frank, R. Barbieri, V. Solo, and E. N. Brown, "Dynamic analysis of neural encoding by point process adaptive filtering," *Neural Computation,* vol. 16, pp. 971-998, May 2004.

[7] U. T. Eden, W. Truccolo, M. R. Fellows, J. P. Donoghue, and E. N. Brown, "Reconstruction of hand movement trajectories from a dynamic ensemble of spiking motor cortical neurons," in *Engineering in Medicine and Biology Society, 2004. IEMBS '04. 26th Annual International Conference of the IEEE*, 2004, pp. 4017-4020.

[8] R. H. M. Chan, D. Song, and T. W. Berger, "Tracking Temporal Evolution of Nonlinear Dynamics in Hippocampus using Time-Varying Volterra Kernels," *2008 30th Annual International Conference of the IEEE Engineering in Medicine and Biology Society, Vols 1-8,* pp. 4996-4999, 2008.

[9] R. H. M. Chan, D. Song, and T. W. Berger, "Nonstationary Modeling of Neural Population Dynamics," *Embc: 2009 Annual International Conference of the Ieee Engineering in Medicine and Biology Society, Vols 1-20,* pp. 4559-4562, 2009.

[10] R. E. Hampson, J. D. Simeral, and S. A. Deadwyler, "Distribution of spatial and nonspatial information in dorsal hippocampus," *Nature,* vol. 402, pp. 610-614, Dec 9 1999.

[11] R. H. M. Chan, D. Song, A. V. Goonawardena, S. Bough, J. Sesay, R. E. Hampson, S. A. Deadwyler, and T. W. Berger, "Changes of Hippocampal CA3-CA1 Population Nonlinear Dynamics across Different Training Sessions in Rats Performing a Memory-Dependent Task," in *32nd Annual International Conference of the IEEE EMBS*, 2010, pp. 5464-5467.